

Black Holes and Wormholes in 2+1 Dimensions*

Dieter Brill[†]

University of Maryland, College Park, MD 20742, USA

and

Albert-Einstein-Institut, Potsdam, FRG

Abstract

Vacuum Einstein theory in three spacetime dimensions is locally trivial, but admits many solutions that are globally different, particularly if there is a negative cosmological constant. The classical theory of such locally “anti-de Sitter” spaces is treated in an elementary way, using visualizable models. Among the objects discussed are black holes, spaces with multiple black holes, their horizon structure, closed universes, and the topologies that are possible.

1 Introduction

On general grounds (2+1)-dimensional spacetime was considered unlikely to support black holes, before such solutions were discovered [1]. Black holes were commonly conceived as places where the effects of gravity are large, surrounded by a region where these effects are asymptotically negligible. Another possible reason is the idea that black holes are “frozen gravitational waves” and therefore exist only in a context where the gravitational field can have independent degrees of freedom. In 2+1 dimensional Einstein theory — that is, Einstein’s equations in a 3-dimensional space-time of signature $(-++)$ — the pure, sourceless gravitational field has no local degrees of freedom, because in three dimensions the Riemann tensor is given algebraically by the Einstein tensor, which in turn is algebraically determined by the Einstein field equations. If there is no matter source and no cosmological constant, the Riemann tensor vanishes and spacetime is flat; if there is no matter but a cosmological constant Λ , the Riemann tensor is that of a space of constant curvature $\Lambda/3$. Thus gravity does not vary from place to place and it does not have any wave degrees of freedom. These were some of the reasons why the possibility of black holes was discounted, and the discovery of black hole solutions in 2+1 D spacetimes with a negative Λ came as such a surprise.

*to appear in Proceedings of 2nd Samos Meeting on Cosmology Geometry and Relativity, Springer-Verlag

[†]email:brill@physics.umd.edu

The existence of (2+1)-dimensional black holes of course does not alter the absence of gravitational waves in (2+1)-dimensional Einstein spaces, nor the lack of variation of their curvature. The curvature of spacetimes satisfying the sourceless Einstein equations with negative Λ is constant negative, and the asymptotic region does not differ locally from the geometry near the black hole. Indeed, black hole solutions can be obtained from the standard, simply connected spacetime of constant negative curvature (anti-de Sitter space, AdS space for short) by forming its quotient space with a suitable group of isometries.¹ One of the criteria on the isometries is that the quotient space should not have any objectionable singularities. For example, if the group contains isometries of the rotation type, with a timelike set of fixed points, then the quotient space will have singularities of the conical kind. Such singularities can represent “point” particles, and the corresponding spacetime can be interpreted as an interesting and physically meaningful description of the dynamics of such particles [4]. However, we confine attention to solutions of the sourceless Einstein equations with negative cosmological constant — whether black holes or not — that are at least initially nonsingular. Therefore we exclude such particle-like solutions. (Likewise, we will not consider the interesting developments in lower-dimensional dilaton gravity, nor other matter fields [5].)

On the other hand, the group used to construct our quotient space may have isometries that are locally Lorentz boosts, with spacelike sets of fixed points. The corresponding singularities are of the non-Hausdorff “Misner” type [6]. If such a singularity does not occur on an initial spacelike surface, and is hidden behind an event horizon, then the spacetime can be acceptable as a representation of a black hole. Finally, the isometry may not have any fixed points but still lead to regions in the quotient space that are to be considered singular for physical reasons, and such regions may again be surrounded by an event horizon, yielding other types of black holes.

Thus the proper criterion characterizing a black hole in this context is not a region of large curvature or an infinite red shift (in typical representations of AdS space itself, where there is no black hole, there is an infinite red shift between the interior and the region near infinity), but existence of an event horizon. This in turn requires the existence of a suitable \mathcal{S} , whose neighborhood is a region in which “distant observers” can survive for an arbitrarily long time without hitting a singularity. That is, there have to be causal curves (the worldlines of these observers) that can be continued to infinite proper time. For example, Misner space itself — the quotient of Minkowski space by a Lorentz boost — does not satisfy this criterion in any dimension, because all timelike curves intersect the non-Hausdorff singularity in a finite proper time. Thus the case $\Lambda = 0$ does not yield any black holes. The same is true, for similar reason, in the case $\Lambda > 0$. However, for $\Lambda < 0$ the situation is different: there are worldlines along which observers can survive forever in an AdS environment. Thus our black holes will not be asymptotically flat [7], but asymptotically AdS. We will see (in section

¹It appears that all locally AdS spacetimes can be obtained in this way [2]. This is not so for positive curvature [3].

3) that the usual definition of black holes can be applied to these spacetimes, and even before we have come to this we will speak of them as black holes.

We can understand the difference between the cases $\Lambda \geq 0$ and $\Lambda < 0$ as a consequence of the positive “relative acceleration” of spacelike geodesics in spaces of negative curvature. In three dimensions, $\Lambda < 0$ implies constant negative curvature. Spacelike geodesics reaching the asymptotically AdS region will therefore increase their separation without limit. The fixed points of the identification that generates a black hole — that is, the “singularities” — lie along a spacelike geodesic. Consider a set of observers located initially further and further towards the asymptotic region and along another spacelike geodesic, which does not intersect the geodesic of fixed points. The timelike distance of an observer from the singularity will then eventually increase without limit, so a sufficiently far-out observer can survive for an arbitrarily long time.

We note in passing that *timelike* geodesics in spacetimes of constant negative curvature have the opposite property: they accelerate toward each other. Thus $\Lambda < 0$ corresponds to a universal “attractive” gravity, and a black hole in such a spacetime exerts this same attraction on test particles, as a black hole should.

The quotient of the anti-de Sitter universe with the group generated by a single finite isometry that is without fixed points, at least on some initial spacelike surface, yields a single black hole, called a BTZ spacetime (for its discoverers, Bañados, Teitelboim and Zanelli [1]). As we will see, one can quotient a BTZ spacetime by another isometry, obtaining more complicated black holes, and this process can be repeated an arbitrary number of times. Although the isometries used cannot be entirely arbitrary, the variety of possibilities and of the resulting spacetimes is quite large. These spacetimes cannot be described by their metric in one or in a few simple coordinate systems, because many coordinate patches would be needed to cover their possibly complicated topology. In principle such a spacetime is of course defined, and all its physical properties are computable, once we know the structure of the isometries that generate it. But such a presentation does not give an accessible and easily visualizable picture of the spacetime. Therefore we prefer to describe the spacetimes combinatorially, by “gluing together” pieces of anti-de Sitter space. This view allows one to gain many important geometrical insights directly, without much algebra or analysis (even if a few of these geometrical constructions may resemble a tour de force).

In section 2 we consider the simplest, time-symmetric case. Because the extrinsic curvature of the surface of time-symmetry vanishes, this surface is itself a smooth two-dimensional Riemannian space of constant negative curvature. This class of spaces has been studied in considerable detail [8]. In particular, almost all two-dimensional spacelike topologies occur already within this class. Section 3 considers the time development of these spaces; we find that all the non-compact initial states develop into black holes. The horizon can be found explicitly, although its behavior can be quite complicated.

Section 4 concerns spacetimes that are not time-symmetric but have angular momentum.

An important reason for studying the classical behavior of these spacetimes is their relative simplicity while still preserving many of the features of more

realistic black hole spacetimes. They are therefore interesting models for testing the formalism of quantum gravity. We do not go into these developments but refer the reader to the recent book by S. Carlip [9].

2 Time-symmetric geometries

Three-dimensional AdS space has many totally geodesic (“time-symmetric”) spacelike surfaces. Because the extrinsic curvature of such surfaces vanishes, they have constant negative curvature Λ . Each such surface remains invariant under a “little group” of AdS isometries, which are therefore isometries of the spacelike surface, and conversely each isometry of the spacelike surface can be extended to be an isometry of the whole AdS spacetime.² Therefore any identification obtained by isometries on the spacelike surface can likewise be extended to the whole spacetime. (AdS space identified by this extension coincides with the usual time development of the initial data via Einstein’s equations where the latter is defined, but it even goes beyond any Cauchy horizon). Thus to identify the possible time-symmetric geometries it suffices to discuss the possible initial spacelike geometries — although this leaves the time development still to be made explicit.

2.1 Coordinates

Although most physically and mathematically interesting facts about constant negative curvature spaces can be phrased without reference to coordinates, and even usefully so, it is convenient for the elucidation and proof of these facts to have coordinates available. Because of the large number of symmetries of AdS spacetime, its geometry takes a simple form in a large number of coordinate systems, which do not usually cover all of the spacetime, but which exhibit explicitly one or several of these symmetries. The simplest coordinates are the redundant set of four X^μ , $\mu = 1, \dots, 4$ in terms of which AdS space is usually defined, namely as an embedding in four-dimensional flat space with signature $(-, -, +, +)$ and metric

$$ds^2 = -dU^2 - dV^2 + dX^2 + dY^2 \tag{1}$$

by the surface

$$-U^2 - V^2 + X^2 + Y^2 = -\ell^2. \tag{2}$$

This spacetime is periodic in the timelike direction with the topology $S^1 \times R^2$; for example, for $X^2 + Y^2 < \ell^2$ the curves $(X, Y) = \text{const}$, $U^2 + V^2 = \ell^2 - X^2 - Y^2$ are closed timelike circles. In the following we assume that this periodicity has been

²Since AdS spacetime is an analytic continuation (both in signature and curvature) of the familiar spherical geometry, such properties can be considered extensions of the corresponding statements about spheres, mutatis mutandis for the difference in group structure, $\text{SO}(4)$ vs $\text{SO}(2,2)$. Analogous statements are true about surfaces of constant extrinsic curvature.

removed by passing to the universal covering space with topology R^3 , which we will call AdS space. If it is necessary to distinguish it from the space of Eq (2) we will call the latter “periodic AdS space.” Either spacetime is a solution of the vacuum Einstein equations with a negative cosmological constant $\Lambda = -1/\ell^2$.

Eq (2) shows that AdS space is a surface of constant distance from the origin in the metric (1). It therefore inherits from the embedding space all the isometries that leave the origin fixed, which form the $SO(2,2)$ group. AdS space can be described by coordinates analogous to the usual spherical polar coordinates as in Eq (9), but of greater interest are coordinates related to isometries that leave a plane fixed, and whose orbits lie in the orthogonal plane. These have the nature of rotations if the plane is spacelike (or double-timelike, such as the (U, V) plane), and of Lorentz transformations if the plane is timelike. Isometries corresponding to orthogonal planes commute, and we can find coordinates that exhibit such pairs of isometries explicitly. If the isometries are rotations, the coordinates cover all of AdS space; if they are Lorentz transformations the corresponding coordinates are analogous to Rindler coordinates of flat space, and need to be analytically extended in the usual fashion to cover all of the spacetime.

For example, if we choose rotations by an angle θ in the (X, Y) plane and by an angle t/ℓ in the (U, V) plane, and specify the respective orbits on the AdS surface by

$$U^2 + V^2 = \ell^2 \cosh^2 \chi \quad \text{and} \quad X^2 + Y^2 = \ell^2 \sinh^2 \chi$$

(so that, for example, $U = -\ell \cosh \chi \cos \frac{t}{\ell}$, $V = \ell \cosh \chi \sin \frac{t}{\ell}$) we obtain the metric

$$ds^2 = -\cosh^2 \chi dt^2 + \ell^2 (d\chi^2 + \sinh^2 \chi d\theta^2). \quad (3)$$

In order to describe the universal covering space we have to allow t to range $-\infty < t < \infty$, whereas θ has its usual range, $0 \leq \theta < 2\pi$, and similarly $0 \leq \chi < \infty$. Except for the usual polar coordinate singularity at $\chi = 0$, these coordinates cover all of AdS space by a sequence of identical (“static”) two-dimensional spacelike surfaces $t = \text{const}$ having a standard metric of spaces of constant negative curvature $-1/\ell^2$. Because $U = 0 = V$ does not occur on (2), shifts in the t coordinate are true translations, without fixed points. These coordinates define timelike sections ($\theta = \text{const}$) and spacelike sections ($t = \text{const}$) of AdS space. Each of these can be represented in a conformal diagram, shown in Fig. 1.

We can define a “radial” coordinate (which really measures the circumference of circles) by

$$r = \ell \sinh \chi.$$

The metric (3) then takes the form

$$ds^2 = -\left(\frac{r^2}{\ell^2} + 1\right) dt^2 + \left(\frac{r^2}{\ell^2} + 1\right)^{-1} dr^2 + r^2 d\theta^2. \quad (4)$$

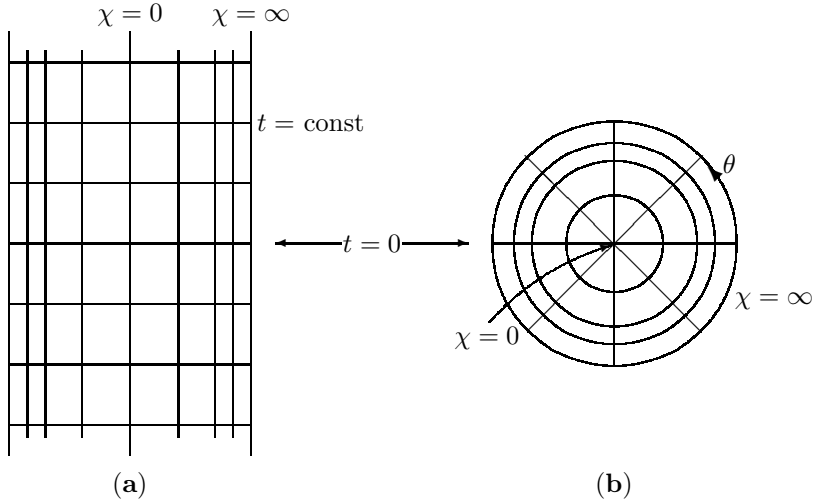


Figure 1: Conformal diagrams of the static (or sausage) coordinates of Eq (3) in sections of AdS space. **(a)** The χ, t section, both sides of the origin. The right half is, for example, $\theta = 0$, and the left half, $\theta = \pi$. **(b)** The section $t = \text{const}$ is the 2D space of constant negative curvature, conformally represented as a Poincaré disk (see section 2.2). The conformal factors are different in the two sections, so they do not represent sections of one three-dimensional conformal diagram. (For the latter see Fig. 4b)

By choosing a new radial coordinate, namely

$$\rho = \ell \tanh \frac{1}{2} \chi$$

to replace the χ of Eq (3), we can make the conformally flat nature of the spacelike section explicit and keep the metric static:

$$ds^2 = - \left(\frac{1 + (\rho/\ell)^2}{1 - (\rho/\ell)^2} \right)^2 dt^2 + \frac{4}{(1 - (\rho/\ell)^2)^2} (d\rho^2 + \rho^2 d\theta^2). \quad (5)$$

A picture like Fig. 1, with parts **(a)** and **(b)** put together into a 3-dimensional cylinder, can be considered a plot of AdS space in the cylindrical coordinates of Eq (5). Because of the cylindrical shape of this diagram these coordinates are sometimes called *sausage coordinates* [10]. Like the static coordinates of (3), these cover all of AdS space.

If we follow an analogous construction but use the timelike (X, U) and (Y, V) planes with orbits (in terms of a new coordinate χ)

$$-V^2 + X^2 = -\ell^2 \cosh^2 \chi \quad \text{and} \quad -U^2 + Y^2 = \ell^2 \sinh^2 \chi,$$

and new hyperbolic coordinates ϕ and t/ℓ , we obtain the metric

$$ds^2 = -\sinh^2 \chi dt^2 + \ell^2 (d\chi^2 + \cosh^2 \chi d\phi^2). \quad (6)$$

By defining

$$r = \ell \cosh \chi$$

we can change this to the Schwarzschild-coordinate form

$$ds^2 = -\left(\frac{r^2}{\ell^2} - 1\right) dt^2 + \left(\frac{r^2}{\ell^2} - 1\right)^{-1} dr^2 + r^2 d\phi^2, \quad (7)$$

which is usually derived from the “rotationally” symmetric ansatz — however, in this description of AdS space, ϕ has to be given the full range, $-\infty < \phi < \infty$ of a hyperbolic angle. The range of r for which the metric (7) is regular, $\ell < r < \infty$, describes only a part of ads space, as can be seen from the explicit expression for the embedding in terms of these coordinates,

$$\begin{cases} U = (r^2 - \ell^2)^{1/2} \sinh \frac{t}{\ell} \\ V = r \cosh \phi \\ X = r \sinh \phi \\ Y = (r^2 - \ell^2)^{1/2} \cosh \frac{t}{\ell} \end{cases} \quad (8)$$

This regular region can be patched together in the usual way with the region $0 < r < \ell$ (Fig. 2), to describe a larger part of AdS space. But if it is desired (for whatever bizarre reason) to describe all of AdS space by analytic extensions of the coordinates (8), one needs also analytic extensions beyond the null surfaces $\phi = \pm\infty$ (or $r = 0$), which are quite analogous to the usual Schwarzschild-type “horizon” null surfaces $t = \pm\infty$ (or $r = \ell$). One then finds two disjoint regions of a third type (not shown in the Figure because they extend perpendicular to the plane of Fig. 2a) in which r^2 is negative and ϕ is the timelike coordinate.³

Another interesting coordinate system is closely related to ordinary polar coordinates on the three-sphere:

$$\begin{cases} U = \ell \sin \frac{\tau}{\ell} \\ V = (r^2 - \ell^2)^{1/2} \cos \frac{\tau}{\ell} \\ X = r \cos \frac{\tau}{\ell} \cos \phi \\ Y = r \cos \frac{\tau}{\ell} \sin \phi \end{cases} \quad (9)$$

with the metric

$$ds^2 = -d\tau^2 + \cos^2 \left(\frac{\tau}{\ell}\right) \left[\left(\frac{r^2}{\ell^2} - 1\right)^{-1} dr^2 + r^2 d\phi^2 \right]. \quad (10)$$

³Like all statements derived from embedding equations such as (8) this really applies to periodic AdS space, and should be repeated an infinite number of times for the covering AdS space itself. For example, there are an infinite number of regions of the three types in AdS space.

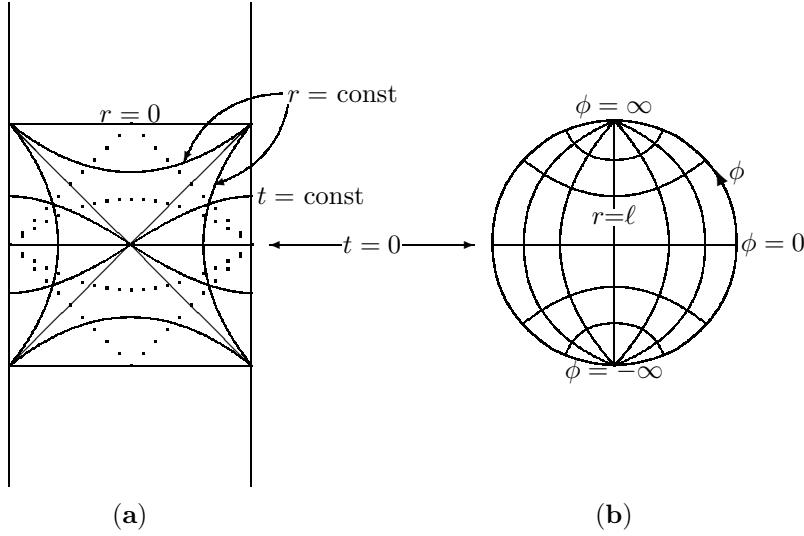


Figure 2: Conformal diagrams of the “Schwarzschild” coordinates of Eq (8) in sections of AdS space. **(a)** An r, t section, continued across the $r = \ell$ coordinate singularity. The outer vertical lines correspond to $r = \infty$. The dotted curves show a few of the surfaces $\tau = \text{const}$ for the coordinates of Eq (10), with limits at $\tau = \pm\pi\ell/2$. **(b)** An r, ϕ section ($r > \ell$) is a two dimensional space of constant negative curvature, conformally represented as a Poincaré disk (see below). The approximately vertical curves are lines of constant r ; they are equidistant in the hyperbolic metric. The approximately horizontal curves are lines of constant ϕ ; they are geodesics in the hyperbolic metric. The outer circle corresponds to $r = \infty$

This is a time development of the same initial values as in (7) (at $t = 0$ resp. $\tau = 0$) but with unit lapse function $N = 1$. The surfaces $\tau = \text{const}$ have constant extrinsic curvature, and they just cover the domain of dependence of those initial values.

Finally one can introduce coordinates that correspond to the flat sections of de Sitter space:

$$\begin{cases} U + Y = r \\ U - Y = r(\phi^2 - t^2) + \frac{1}{r} \\ X = r\phi \\ V = rt \end{cases} \quad (11)$$

The metric then takes the form

$$ds^2 = -r^2 dt^2 + \frac{dr^2}{r^2} + r^2 d\phi^2. \quad (12)$$

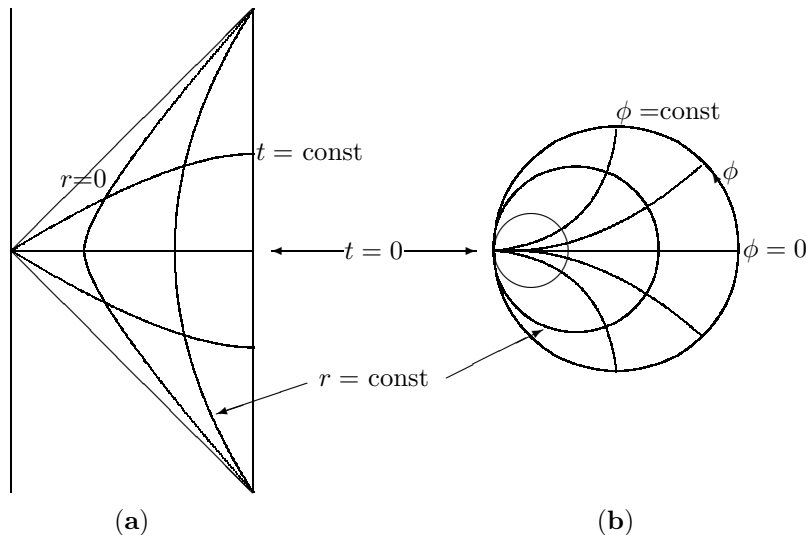


Figure 3: Conformal diagram of the “extremal” Schwarzschild coordinates of Eq (11) in sections of AdS space. **(a)** An r, t section. **(b)** An r, ϕ section. The lines $r = \text{const}$ are *horocycles* of the Poincaré disk.

Here the $r = \text{const}$ sections are manifestly flat.⁴ Fig. 3 shows the conformal picture of these coordinates.

The spacelike surfaces $t = \text{const}$ are conformally flat as are all two-dimensional surfaces, and as is manifest in Eq (5). Less trivially, the three-dimensional AdS spacetime also has this property, so neighborhoods of AdS space can be conformally mapped to flat space (one of the few cases where a three-dimensional conformal diagram exists). Such a map is the “stereographic” projection, a projection by straight lines in the embedding space from a point in the surface of Eq (2) onto a plane tangent to that surface at the antipodal point, analogous to the familiar stereographic projection of a sphere (Fig. 4a). By projection from the point $(U, V, X, Y) = (-\ell, 0, 0, 0)$ to the plane $U = \ell$ we obtain the coordinates (provided $U > -\ell$)

$$x^\mu = \frac{2\ell X^\mu}{U + \ell} \quad X^\mu \neq U \quad (13)$$

with the metric (where $X^0 = V, x^0 = t$)

$$ds^2 = \left(\frac{1}{1 - r_c^2} \right)^2 (-dt^2 + dx^2 + dy^2) \quad \text{where} \quad r_c^2 = \frac{-t^2 + x^2 + y^2}{4\ell^2}. \quad (14)$$

This metric is time-symmetric about $t = 0$ but not static. It remains invariant under the Poincaré group of the flat 2+1-dimensional Minkowski space (t, x, y).

⁴These subspaces are the analog in the case of Lorentzian metrics of *horospheres* of hyperbolic spaces (see, for example, [8]).

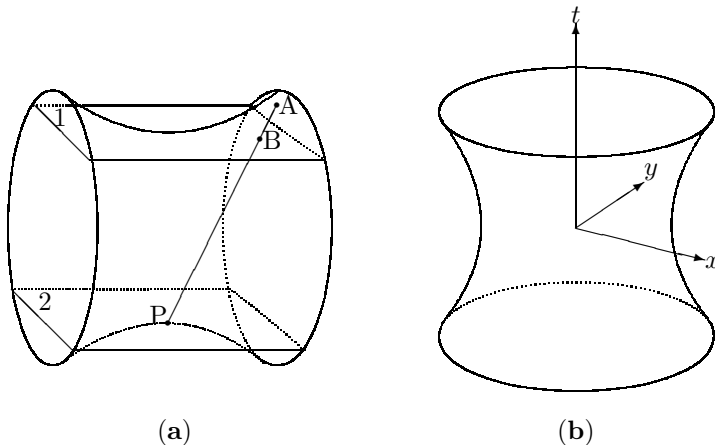


Figure 4: AdS space in stereographic projection. (a) The hyperboloid is 2-dimensional AdS space embedded in 3-dimensional flat space as in Eq (2), restricted to $Y = 0$. It is projected from point P onto the plane 1 ($U = \ell$). The image of point A in the hyperboloid is point B in the plane. The part of the hyperboloid that lies below plane 2 is not covered by the stereographic coordinates. (b) When plotted in the stereographic coordinates (13), AdS space is the interior of a hyperboloid. The boundary of the hyperboloid is (part of) the conformal boundary of AdS space.

In particular the origin may be shifted and the projection “centered” about any point in AdS space (by projecting from the corresponding antipodal point).

Because of the condition $U > -\ell$ the stereographic projection fails to cover a part of AdS space, even in the periodically identified version (Fig. 4a). The 3-dimensional conformal diagram is the interior of the hyperboloid $r_c = 1$, where the conformal factor of the metric (14) is finite (Fig. 4b). On the surface of time-symmetry, $t = 0$, the stereographic metric agrees with the sausage metric (5).

Many similar coordinate systems, illustrating various symmetries of AdS space, are possible; for examples see [11].

2.2 Isometries and Geodesics

To discuss the identifications that lead to time-symmetric black holes and other globally non-trivial 2+1-dimensional solutions we need a convenient representation of isometries and other geometrical relations in a spacelike initial surface of time-symmetry. Such a representation is the conformal map of Figs 1 and 2, in which this spacelike surface is shown as a disk, known as the *Poincaré disk*. This representation has been extensively studied (see, for example, [8]), and we only mention the features that are most important for our task.

All totally geodesic, time-symmetric surfaces H^2 in AdS space are isometric

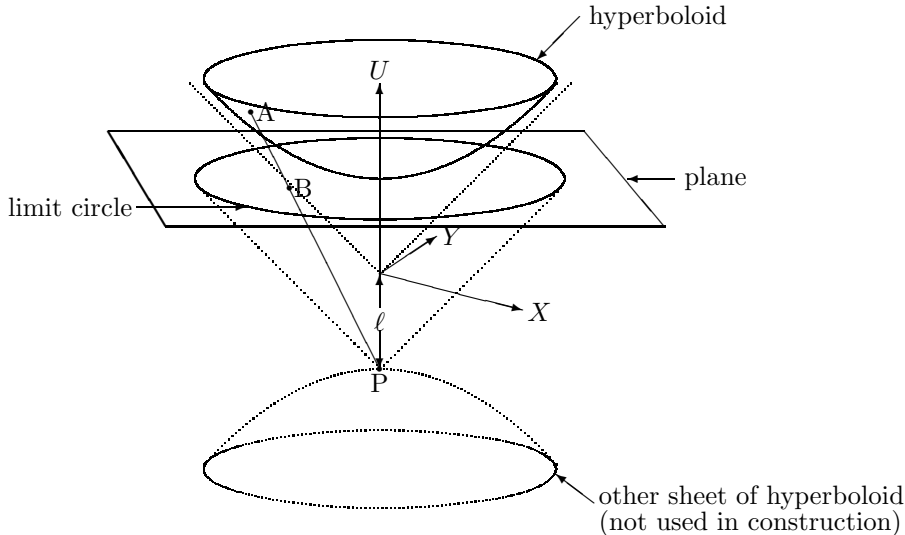


Figure 5: The two-dimensional space H^2 of constant curvature $1/\ell^2$ is embedded in flat Minkowski space as one sheet of the hyperboloid of Eq (15). Under a stereographic projection from point P to the plane, point A on the hyperboloid is mapped to point B in the plane. Thus the hyperboloid (H^2) is mapped onto the Poincaré disk, the interior of the curve marked limit circle

to the typical hyperboloid (Fig. 5) obtained by restricting Eq (2) to $V = 0$,

$$X^2 + Y^2 - U^2 = -\ell^2 \quad (15)$$

This surface has zero extrinsic curvature and therefore constant negative Gaussian curvature $-1/\ell^2$. The Poincaré disk can be obtained as a map of H^2 by the stereographic projection of Fig. 5, which illustrates Eq (13) when restricted to $V = 0$ similar to the way Fig. 4 illustrates it when restricted to $X = 0$. In this way all of H^2 is mapped into the interior of a disk of radius 2ℓ , whose boundary, called the limit circle, represents points at (projective or conformal) infinity. Because the map is conformal, angles are faithfully represented. Other geometrical objects in H^2 appear distorted in the Euclidean geometry of the disk, but by assigning new roles to these “distorted” objects and manipulating those according to Euclidean geometry one can perform constructions equivalent to those in the H^2 -geometry directly on the Poincaré disk.

For example, on the surface H^2 as described by Eq (15), all geodesics are intersections of planes through the origin with the surface; that is, they satisfy a linear relation between X, Y, U . From Eq (13) it follows directly that Eq (15) becomes such a linear relation if x, y satisfy the equation of a circle that has radius $(a^2 - 4\ell^2)$ if it is centered at $(x, y) = (a_x, a_y)$, hence meets the limit circle at right angles. Because two such circles intersect in at most one point in the interior of the Poincaré disk, it follows that two geodesics in H^2 meet at most in one point (as in Euclidean space).

An important difference occurs if two geodesics do *not* meet: in Euclidean space they are then equidistant; whereas in the Poincaré disc the geodesic between points on two disjoint geodesics (Euclidean circles perpendicular to the limit circle) approaches a complete geodesic as the points approach the limit circle. The length of such a complete geodesic is infinite, since the conformal factor in the metric of Eq (14), restricted to $t = 0$,

$$ds^2 = \left(1 - \frac{x^2 + y^2}{4\ell^2}\right)^{-2} (dx^2 + dy^2) \quad (16)$$

increases without limit as $x^2 + y^2 \rightarrow 4\ell^2$. Hence on H^2 the geodesic distance between two given disjoint geodesics typically increases without bound as we go along the given geodesics in either direction. It is therefore reasonable, as can be shown, that the geodesic distance between points on two given disjoint geodesics has a lower bound, and if this is nonzero there is a unique geodesic segment of minimal length joining the two given geodesics at right angles to either.

On the other hand, if we have a family of equidistant curves, at most one of them can be a geodesic, and then the representation of the others on the Poincaré disk are (arcs of) circles, not perpendicular to the limit circle, but meeting the geodesic asymptotically at the limit circle. The curves $r = \text{const}$ of Fig. 2b are examples, with $r = \ell$ the geodesic of the family. These equidistant curves have constant acceleration (with respect to their arclength parameter), and they also illustrate how the conformal factor in (16) distorts the apparent (Euclidean) distances of the disk into the true distances of H^2 .

Because the surface (15) in Minkowski space has constant extrinsic curvature, any isometry of the surface geometry can be extended to an isometry of the embedding space. But we know all those isometries: they form the homogeneous isochronous Lorentz group. Thus any Lorentz transformation implies, by the projection of Fig. 5, a corresponding transformation of the Poincaré disk that represents an isometry of H^2 , and all H^2 isometries can be obtained in this way. In the Euclidean metric of the disk such transformations must be conformal transformations leaving the limit circle fixed, since they are isometries of the conformal metric (16).

Knowing this we can now classify⁵ the isometries of H^2 . Proper Lorentz transformations in 3D Minkowski space have an axis of fixed points that may be a spacelike, null, or timelike straight line. If the axis is timelike, it intersects the hyperboloid (15). If the axis is null, it intersects the hyperboloid asymptotically. If the axis is spacelike, it does not intersect the hyperboloid, but there are two fixed null directions perpendicular to the axis. Correspondingly on the Poincaré disk there is either one fixed point within the disk (“elliptic”), or one fixed point on the limit circle (“parabolic”), or two fixed points on the limit circle (“hyperbolic”) for these transformations. Fig. 1b illustrates by the transformation $\theta \rightarrow \theta + \text{const}$ the case with one finite fixed point (the origin).

⁵We confine attention to orientation-preserving transformations; they can be combined with a reflection about a geodesic (with an infinite number of fixed points) to obtain the rest.

Figs. 2b and 3b illustrate by the transformation $\phi \rightarrow \phi + \text{const}$ the case with two fixed points and one fixed point, respectively, on the limit circle ($\phi = \pm\infty$). In the case of two fixed points there is a unique geodesic ($r = \ell$ in Fig. 2b) left fixed by the isometry, and conversely the isometry, which we will call “along” the geodesic, is uniquely defined by the invariant geodesic and the distance by which a point moves along that geodesic.

Except for the rotation about the center of the disk as in Fig. 1b these are not isometries of the disk’s flat, Euclidean metric, but they are of course conformal isometries of this metric. Such conformal transformations, mapping the limit circle into itself, are conveniently described as *Möbius transformations* of the complex coordinate

$$z = \frac{x + iy}{\ell} \quad \text{by} \quad z \rightarrow z' = \frac{az + b}{\bar{b}z + \bar{a}}, \quad (17)$$

where a, b are complex numbers with $|a|^2 - |b|^2 = 1$. When we consider an isometry or identification abstractly, it can always be implemented concretely by such a Möbius transformation. In particular, hyperbolic isometries are described by Möbius transformations with real a .

As the examples of Figs. 1-3 show, each of these isometries is part of a family depending on a continuous parameter (the constant in $\phi \rightarrow \phi + \text{const}$, for example). There is therefore an “infinitesimal” version of each isometry, described by a Killing vector ($\partial/\partial\phi$ in the example). Conversely an isometry can be described as the exponential of its Killing vector.

2.3 Identifications

The hyperbolic transformations, which have no fixed points in H^2 , are suitable for forming nonsingular quotient spaces that have the same local geometry as AdS space, and hence satisfy the same Einstein equations. In the context of Fig. 2b and Eq (7) the transformation that comes to mind is described by $\phi \rightarrow \phi + 2\pi$. The quotient space is the space in which points connected by this transformation are regarded as identical, which is the same as the space in which ϕ is a periodic coordinate with the usual period. Eq (7) with this periodicity in ϕ already gives us the simplest BTZ metric for a single, non-rotating 2+1-dimensional black hole.

The minimum distance between the two identified geodesics occurs at $r = \ell$ and is $2\pi\ell$. After identification this is the minimum distance around the black hole, and plays the role of the horizon “area”. If we identify ϕ with a different period $2\pi a$, we get a metric with a different horizon size. We can then redefine the coordinates so that ϕ has its usual period,

$$\phi \rightarrow a\phi, \quad r \rightarrow r/a \quad t \rightarrow at$$

and the metric takes this standard form, called the BTZ metric [1]

$$ds^2 = - \left(\frac{r^2}{\ell^2} - m \right) dt^2 + \left(\frac{r^2}{\ell^2} - m \right)^{-1} dr^2 + r^2 d\phi^2, \quad (18)$$

where $m = 1/a^2$. Here the dimensionless quantity m is called the mass parameter. Although it can be measured in the asymptotic region, it is more directly related to the horizon size, the length of the minimal geodesic at the horizon, $2\pi\ell\sqrt{m}$.

The metric (18) is a solution also for $m = 0$, as shown by Eq (12), but that is not the AdS metric itself. The latter is also described by Eq (18), but with $m = -1$, as shown by Eq (4). By contrast, the $m = 0$ initial state is obtained by identifying the geodesics $\phi = 0$ and $\phi = 2\pi$ in Fig. 3b.

To describe the identification more explicitly, we may say that we have cut a strip from $\phi = 0$ to $\phi = 2\pi$ out of Fig. 2b, and glued the edges together. This strip is a “fundamental domain” for our identification, a region that contains images of its own points under the group only on its boundary, and that together with all its images covers the full AdS space. To obtain a fundamental domain for the BTZ black hole we might have used as the boundaries some other curve on the Poincaré disk and its image under the transformation, provided only that the curve and its image do not intersect. But since it is always possible to avoid apparent asymmetries by choosing boundaries composed of geodesics that meet at right angles, we will generally do so.

We can think of the identification in yet another way, by a process that has been called “doubling”: cut a strip from $\phi = 0$ to $\phi = \pi$ from Fig. 2b, and cut another identical strip. Put one on top of the other and glue the two edges together, obtaining again the black hole initial state. The gluing makes the two strips reflections of each other with respect to either of the original edges. Back on the Poincaré disk the composition of the two reflections is a translation in ϕ by 2π , that is, the isometry of the identification. Any (orientation-preserving) isometry of a hyperbolic space can be decomposed into two reflections [12]; hence any quotient space can be considered the double of a suitable region (possibly in another quotient space), and a fundamental domain is obtained from the region and one of its reflections.

The process of gluing together a constant negative curvature space from a fundamental domain of the Poincaré disk can be reversed: we cut the space by geodesics into its fundamental domain, make many copies of the domain, and put these down on the disk so that boundaries coming from the same cut touch, until the entire disk is covered. The resulting pattern is called a “tiling” of the disk (although the “tiles” corresponding to the $t = 0$ section of the BTZ black hole look more like strip flooring). Thus we have two equivalent ways of describing our identified space: by giving a fundamental domain and rules of gluing the boundaries, or by a tiling together with rules relating each tile to its neighbors.

2.3.1 Tiling and Pythagoras

To fix ideas, consider an application of tiling found among the numerous proofs of the theorem of Pythagoras (a local boy who contributed to the early fame of Samos). This proof is based on the fact that all fundamental domains of a given group of isometries have equal area. In the Euclidean plane we consider

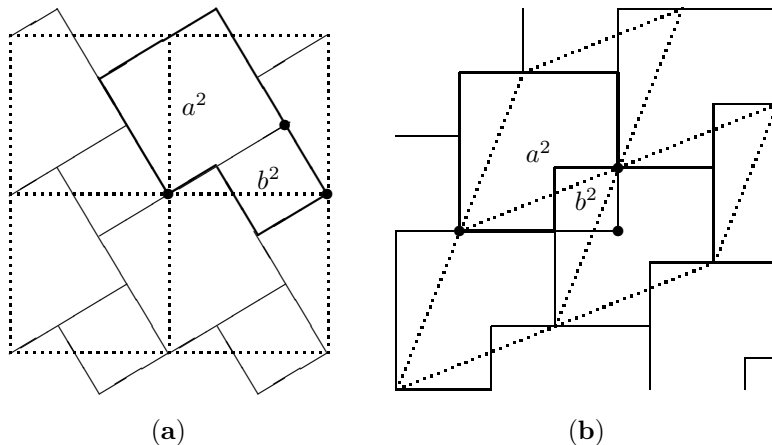


Figure 6: Two different ways of tiling the plane prove the theorem of Pythagoras in (a) Euclidean space and (b) Minkowski space

the group generated by two translations specified in direction and amounts by two adjacent sides of the square above the hypotenuse of a right triangle, whose vertices are the three larger dots in Fig. 6a. This square is a fundamental domain of the group, and part of the tiling by this square is shown by the horizontal and vertical dotted lines. The region drawn in heavy outline is an alternative fundamental domain of the same group of isometries, and that domain is made from the squares above the sides of the same triangle. Part of its tiling of the plane is shown by the lightly drawn lines of Fig. 6a. Either fundamental domain can be glued together to form the same quotient space, a “square” torus, so the areas are equal, $c^2 = a^2 + b^2 = \text{area of torus}$.

In special relativity the theorem of Pythagoras is valid with a different sign, $c^2 = a^2 - b^2$ if we choose the hypotenuse and one of the sides to be spacelike, and of course the right angles of the triangle and of squares are to be drawn in accordance with the Minkowski metric. Fig. 6b shows the proof by the tiling that derives from a Minkowski torus of area c^2 . (Here we use, at least implicitly, the fact that the area of a two-dimensional figure is the same in Euclidean and Minkowski spaces if their metrics differ only by a sign.)

2.3.2 Embeddings

To visualize the geometry of our glued-together surface — the $t = 0$ surface of a static BTZ black hole — it helps to embed this surface in a three-dimensional space in which the gluing can be actually carried out. This is analogous to the embedding of the $t = 0$ surface of the Schwarzschild black hole, with one angle suppressed, in three-dimensional flat space (the surface of rotation of the *Flamm parabola* [13]). For the BTZ initial surface only a finite part can be so embedded. The embedding stops where the rate of increase of circumference of the circle $r = \text{const}$ with respect to the true distance in the radial direction

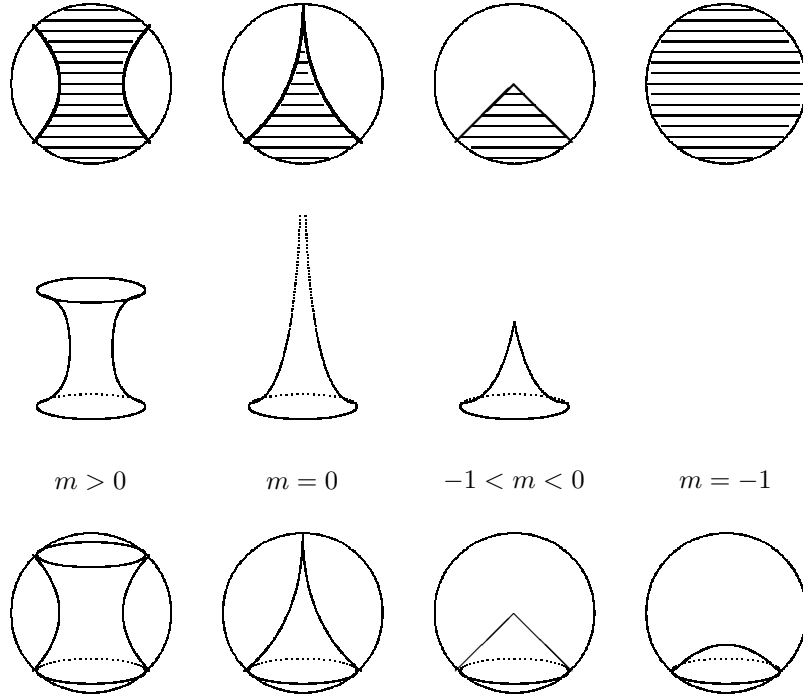


Figure 7: Three representations of the geometry of the $t = 0$ geometry of metric (18) for different ranges of the mass parameter m : The BTZ black hole for $m > 0$; the extremal BTZ black hole for $m = 0$; the point particle (conical singularity) for $m < 0$; and AdS (“vacuum”) space itself for $m = -1$. **Top row:** shaded regions of the Poincaré disk, to be identified in each figure along the left and right boundaries, drawn in thicker lines. **Second row:** an embedding of the central part ($r \leq \ell\sqrt{1-m}$) of these spaces as surfaces in three-dimensional flat Euclidean space. The embedding cannot be continued beyond the outer edges of each figure. **Bottom row:** the entire surface can be embedded in a 3D space of constant negative curvature, shown as a Poincaré ball. (The figure is schematic only; for example, the angle at the conical tips ought to be the same in the second and last row, to represent the same surface)

exceeds that rate in flat space. (The remainder of the surface could then be embedded in Minkowski space, but the switch between embeddings is an artifact and corresponds to no local intrinsic property.) However, the entire surface can be embedded in H^3 , the *Riemannian* (positive definite metric) space of constant negative curvature. By the obvious generalization of the Poincaré disk this space can be conformally represented as a ball in three-dimensional flat space. Fig. 7 shows this embedding, where the surface for $m > 0$ is seen to have two asymptotic sheets, similar to the corresponding Schwarzschild surface.

2.4 Multiple Black Holes

We saw that a single hyperbolic isometry (call it a) used as an identification to obtain an AdS initial state always yields a (single) BTZ black hole state, with horizon size and location depending on a . For other types of initial states we therefore need to use more than one such isometry, for example a and b . Assuring that there are no fixed points (which would lead to singularities of the quotient space) would then seem to be much more difficult: If we know that a has no fixed point, then the whole group consisting of powers a^n has no fixed points (except the identity, $n = 0$); but for the group generated by two isometries a, b we have to check that no “word” formed from these and their inverses, such as $ab^{-2}a^3b$ has fixed points. Although this may seem complicated, it is easy if we have a fundamental domain such that the isometry a maps one of a pair of boundaries into the other, and the isometry b does the same for a different pair of boundaries. Now tile the Poincaré disk with copies of this fundamental domain (see Fig. 10 for an example). Once we fix the original tile (associated with the identity isometry), there is a one-to-one correspondence between tiles and words. Therefore every non-trivial word moves all points in the original tile to some different tile, and there can be no fixed points in the open disk.

How to obtain such a fundamental domain? A simple way is by doubling a region bounded by any number k of non-intersecting geodesics [14]. Fig. 8a shows this for the case $k = 3$. In Fig. 8b we see the fundamental domain. Half of it is the original (heavily outlined) region, shifted to the right so that the center of the Poincaré disk lies on the geodesic boundary of the region rather than at its center. The other half is the reflection of this original region across that geodesic boundary. Thus $2k - 2 = 4$ boundaries remain to be identified in pairs, as indicated in the figure for the top pair. To construct the isometry that moves one member of such a pair into the other we find the unique common normal geodesic H_2 (shown for the bottom pair), and its intersection with the limit circle; these intersections are the fixed points of one of the hyperbolic isometries that have this fundamental domain. For example, in Fig. 8b the isometry associated with H_2 moves one of the bottom boundaries into the other. Similarly we find $k - 2$ other isometries, each of them associated with a common normal. After the identification are made these common normals are smooth closed geodesics that separate an asymptotically AdS region from the rest of the manifold. We call such curves horizons. In addition to the $k - 1$ horizons found

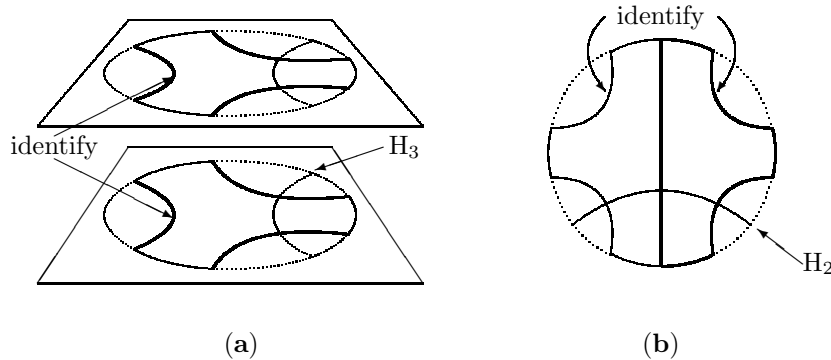


Figure 8: Initial state for an AdS spacetime containing three black holes. (a) Representation by doubling a region on the Poincaré disk. The top and bottom surfaces are to be glued together along pairs of heavily drawn curves, such as the pair labeled “identify”. The resulting topology is that of a pair of pants, with the waist and the legs flaring out to infinity at the limit circle. The heavier part of the curve H_3 becomes a closed geodesic at the narrowest part of a leg. (b) The fundamental region, obtained from one of the regions of part (a) by adding its reflection about the geodesic labeled “identify” in (a). In (b) only two boundaries remain to be identified; the top pair are so labeled. For the bottom pair the minimal connecting curve H_2 is shown

this way there is another one, so there is a total of k horizons. The additional one can be found in the above way from a different fundamental domain, obtained by reflecting the original region about a different geodesic boundary, but it is more easily found from the doubling picture, as shown by the H_3 in Fig. 8a.

The topology of the resulting space may be easiest to see in the doubling picture: there are k asymptotically AdS regions, which can be regarded as k punctures (“pants’ legs”) on a 2-sphere. With each asymptotic region there is associated a horizon, namely the geodesic normal to the corresponding adjacent boundaries of the original region (because it is normal it will become a smooth, circular, minimal geodesic after the doubling). On the outside of each horizon the geometry is the same as that obtained from the isometry corresponding to that horizon alone, so it is exactly the exterior of a BTZ black hole geometry. Therefore the whole space contains k black holes, joined together inside each hole’s horizon.

2.4.1 Parameters

The time-symmetric (zero angular momentum) BTZ black hole in AdS space of a given cosmological constant is described by a single parameter, the mass m . For an initial state of several black holes we have analogously the several masses, and in addition the relative positions of the black holes. These are however not all independent. Consider a k black hole initial state obtained by doubling a

simply-connected region bounded by k non-intersecting geodesics. Find the k minimal geodesic segments σ_i between adjacent geodesics.⁶ The parts s_i of the original geodesics between the endpoints of those segments, together with the segments σ_i themselves, form a geodesic $2k$ -gon with right-angle corners. Clearly the σ_i are half the horizon size and hence a measure of the masses, and the s_i may be considered a measure of the distances between the black holes. If $2k - 3$ of the sides of a $2k$ -gon are given, then the geodesics that will form the $2k - 2$ side (orthogonal at the end of the $2k - 3$ side) and the $2k$ side (orthogonal at the end of the first side) are well-defined. They have a unique common normal geodesic that forms the $2k - 1$ side, hence the whole polygon is uniquely defined. Thus only $2k - 3$ of the $2k$ numbers measuring the masses and the distances of this type of multi-black-hole are independent. In the case $k = 3$ (corresponding to a geodesic hexagon) one can show that alternating sides (either the three masses or the three distances) can be *arbitrarily* chosen. Higher $2k$ -gons can be divided by geodesics into hexagons, so at least all the masses (or all the distances) can be chosen arbitrarily. (The remaining $k - 3$ parameters may have to satisfy inequalities.)

Composing the $2k$ -gon out of geodesic hexagons means, for the doubled surface, that the multi-black-hole geometry is made out of $k - 2$ three-black-hole geometries with $2k - 6$ of the asymptotic AdS regions removed and the horizons glued together pairwise. In the five-black-hole example of Fig. 9 the three-black-hole parts are labeled 1, 2, and 3. One asymptotic AdS regions was removed from 1 and 3, and two such regions are missing from 2. The geometries obtained by doubling this are however not the most general time-symmetric multi-black-hole configuration. For example, in Fig. 9 the curve separating regions 2 and 3 is a closed geodesic. If we cut and re-glue after a hyperbolic isometry along this geodesic the geometry is still smooth; the operation amounts to rotating the top and bottom part of Fig. 9b with respect to each other, as indicated by the arrows. That the result is in general different after this rotation is shown, for example, by the change in angle between the boundary geodesic and another closed geodesic which, before the rotation, is indicated by the dotted line in Fig. 9a.

The $2k - 3$ distance parameters and the $k - 3$ rotation angles describe a $3k - 6$ -dimensional space of k -black-hole geometries. Equivalently we may say that a k -black-hole initial state is given by a fundamental domain bounded by $2k - 2$ geodesics to be identified in pairs by $k - 1$ Möbius transformations. Since each Möbius transformation depends on 3 parameters, and the whole fundamental domain can be moved by another Möbius transformation, the number of free parameters is $3k - 6$. Such a space of geometries is known as a Teichmüller space, and the length and twist parameters are known as Fenchel-Nielsen coordinates on this space [8].

Instead of cutting and re-gluing along closed geodesics as in Fig. 9 one can do this operation on the identification geodesics used in the doubling procedure.

⁶Two geodesics of a set are adjacent if each has an end point (at infinity) such that between those end points there is no end point of any other geodesic of the set.

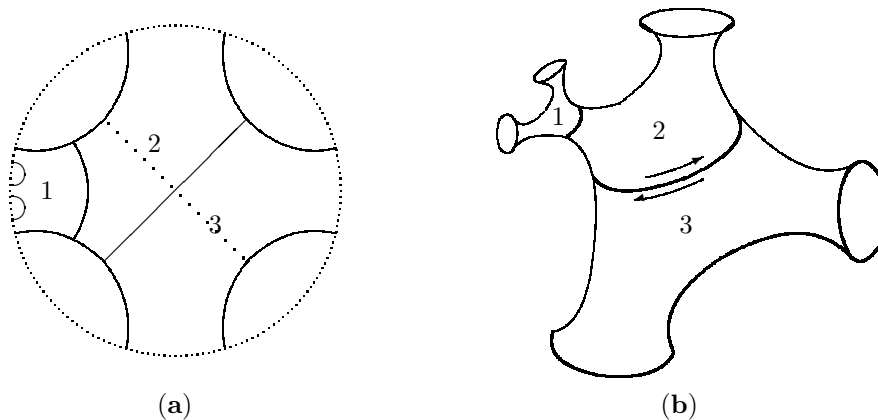


Figure 9: A five-black-hole time-symmetric initial state is obtained by doubling the region on the Poincaré disk in (a). Part (b) shows a somewhat fanciful picture of the result of the doubling, cut off at the flare-outs, which should extend to infinity.

For example, in Fig. 8a on the pair of geodesics marked “identify” one can identify each point on the bottom geodesic with one that is moved by a constant distance along the top geodesic. For the fundamental region this means the following: so far, whenever two identification geodesics on the boundary of the fundamental domain were to be identified, it was done by the unique hyperbolic transformation along the minimal normal geodesic between the identification geodesics. If we follow this transformation by a hyperbolic isometry along one of the identification geodesics, the two geodesics will still fit together, and the identified surface will be smooth but with a difference in global structure (like that produced by the re-gluing in Fig. 9). Of course the two transformations combine into one, and conversely any isometry that maps one identification geodesic into another can be decomposed into a “move” along the normal geodesic, and a “shift” along a identification geodesic. Since each hyperbolic transformation is a Lorentz transformation in the embedding picture (Fig. 5) the combination is again hyperbolic, and no finite fixed points occur in this more general identification process.

If we identify with a non-zero shift, there is of course still a minimal geodesic between the two identified geodesics, but it is no longer orthogonal to those geodesics. Nevertheless the identified geometry is that of a black hole. To make the correspondence to the $\phi \rightarrow \phi + 2\pi$ identification of Eq (7) one would have to change the identification geodesics to be normal to the minimal one (which can complicate the fundamental domain).

2.4.2 Fixed points

It is useful to understand the fixed points at infinity (the limiting circle of the Poincaré disk) of the identifications that glue a black hole geometry out of a fundamental domain of AdS space. The fixed points are directly related to the minimal geodesics associated with the identification, and they can indicate whether we have a black hole or not: there must be open sets free of fixed points if the initial data is to be asymptotically AdS. We know that the identifications can have some fixed points at infinity, but if the fixed points cover all of infinity, there is no place left for an asymptotically AdS region, and the space is not a black hole space. Thus even in the relatively simple time-symmetric case it is useful to understand the tiling and the fixed points of the Möbius transformations of the Poincaré disk associated with the identifications.

As an example, consider again the three-black-hole case. Let a and b be the identifications of the top and the bottom pair of geodesics of a figure like 8b. Then the free group generated by these, that is, any “word” formed from a , b and their inverses A , B is also an identification. Since the identified geometry is everywhere smooth, none of these can have a fixed point in the finite part of the disk, so all fixed points must lie on the limit circle. The pattern of fixed points is characteristic of the identifications and constitutes a kind of hologram of the multi-black-hole spacetime [15].

In Fig. 10 the initial fundamental domain is denoted by $\mathbf{1}$. The identifications are given by hyperbolic Möbius transformations a , b , with inverses A , B that connect the top and the bottom boundaries, respectively. Any “word” made up of these four letters is, first, also an identification. Secondly each word can be used to label a tile, because each tile is some image, $a\mathbf{1}$, $A\mathbf{1}$, $aB\mathbf{1}$, ... of the initial domain $\mathbf{1}$, shown simply as a , A , aB , ... in the Figure. Finally, there is a normal, closed, minimal geodesic associated with each pair of identified geodesics, hence each word also corresponds to a geodesic.⁷ Horizons are special geodesics that are smoothly closed (after the identification is made) and that bound asymptotically AdS regions. Some of these are shown by the heavy curves. The ones that cut through the basic domain are labeled by the isometries that leave them invariant, a , b , and $AB = BA$. The words for the other horizons are obtained from these by conjugation, for example the horizon connecting the points labeled $a(ab)^n$ and $a(BA)^n$ is “called” by the word $a(BA)A$.

Horizon words, being a hyperbolic isometry, have two fixed points on the Poincaré limit circle. We can find the fixed points by applying the word (or its inverse) many times to any finite region, because in the limit the images will converge to a point on the limit circle (see, for example, the equidistant curves in Fig. 2). Some of these fixed points are shown by open and by filled circles in the Figure, and labeled by an n th power, where the limit $n \rightarrow \infty$ is understood. The two fixed points of a hyperbolic transformation define a geodesic that ends at them, and that is the minimal geodesic along which the transformation acts.

Because the infinity side of a horizon is isometric to the asymptotic region

⁷In this connection we regard a word, its inverse, and the permuted word as equal, in order to have a unique correspondence to geodesics; see [16].

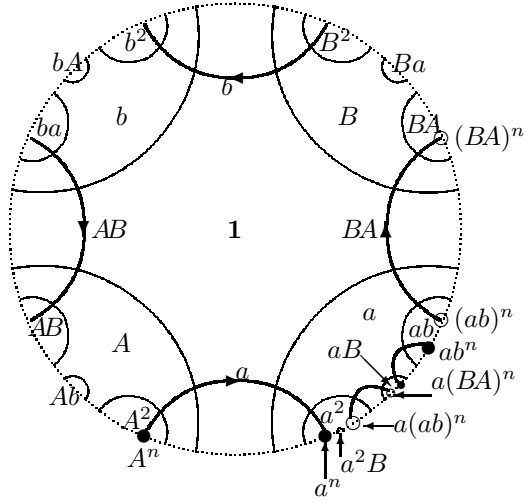


Figure 10: Part of the tiling of the Poincaré disk obtained by “unwrapping” a three-black-hole initial geometry as in Fig. 8. A fundamental domain **1** is imaged by combinations of identification maps a and b and their inverses $A = a^{-1}$, $B = b^{-1}$. Repeating n times a map such as ab leads to a point $(ab)^n$ on the limit circle, in the limit $n \rightarrow \infty$. Some geodesics (“horizons”) connecting such a limit point and its inverse limit (such as $a(ab)^n$ and $a(ab)^{-n} = a(BA)^n$) are shown as heavy curves

of a single black hole, there are no fixed points on that side of the horizon. (Cf. Fig. 2, where the only fixed points of the horizon isometry $\phi \rightarrow \phi + \text{const}$ are on the horizon $r = \ell$.) Between two different horizons (between open and filled circles of the Figure) there will however be further horizons, with fixed points at their ends. Thus the set of fixed points for multi-black-holes has the fractal structure of a Cantor set.

By contrast, for some identifications the fixed points are everywhere dense on the limit circle. This happens, for example, if we try to build, by analogy to the multi-black-hole construction, a geometry containing three $m = 0$ black holes. The tiles, analogs of those of Fig. 10, would be “ideal” quadrilaterals, that is, each tile is a geodesic polygon whose four corners lie on the limit circle. This space is smooth and contains three ends of the type shown in the second column of Fig. 7 (instead of the “legs” in such pictures as Fig. 9); but since there is then no fixed point-free region on the limit circle, this space is not asymptotically AdS and hence does not contain BTZ-type black holes.

2.5 Other Topologies

It is well known that time-symmetric AdS initial states, that is, spaces of constant negative curvature, admit a large variety of topologies. In the context of

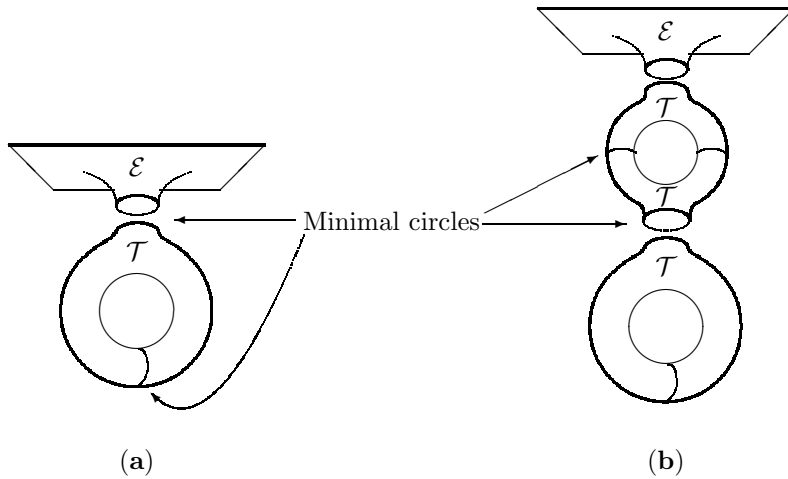


Figure 11: Examples of the class of spaces considered here, constructed by sewing together one or several trousers and one asymptotic region. The latter looks asymptotically flat in this topological picture, but metrically it has constant negative curvature everywhere, just like the trousers

black hole spaces one can construct all of these out of pieces of the three-black-hole space as in Fig. 7. These pieces are three BTZ-exterior, that is, the regions outside each of the three horizons, and the region interior to the horizons. The interior piece is sometimes called the “convex core” or “trousers.”⁸ Fig. 11 shows how other topologies can be constructed out of these pieces.

The resulting geometry is smooth if we choose the freely specifiable mass parameters of each exterior or core to match those of its neighbors at the connection horizons⁹: the intrinsic geometries then match, and the extrinsic geometries match because the horizons are geodesics. Conversely we can decompose a given k -black-hole initial geometry of genus g into asymptotic regions and trousers by cutting it along minimal circles of different and non-trivial homotopy types. We can choose $3g + 2k - 3$ such circles that divide the space into k exteriors \mathcal{E} and $2g + k - 2$ trousers \mathcal{T} . Fig. 11 illustrates the construction for $k = 1$ and $g = 1$ (left) resp. $g = 2$ (right).

A fundamental region on the Poincaré disk, and hence the Möbius transformations that implement the identifications, can be constructed for these spaces in a similar way, by putting together geodesic, right-angle octagons represent-

⁸Previously we have used the image of flared pants’ legs for the asymptotically AdS regions, which need to be cut off to obtain the core, so it would be more consistent to call the latter “cut-offs” or “shorts,” but we will use “trousers.”

⁹The horizons along which the legs were cut off from the cores may no longer be horizons of the space-time if the cores are re-assembled differently. Nonetheless, in the present section we will still call them by that name.

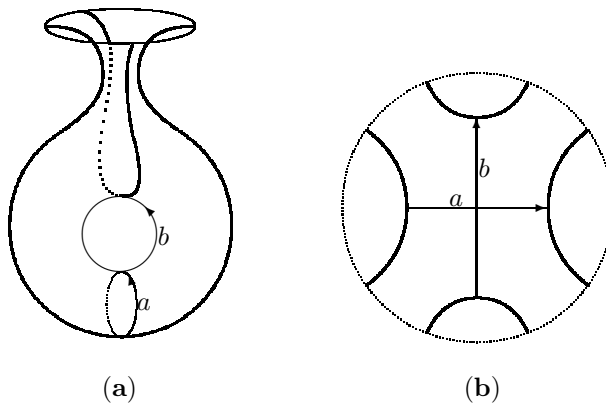


Figure 12: Construction of a BTZ exterior with toroidal interior. Rather than cutting the geometry shown in part **(a)** by minimal geodesics as in Fig. 11, the cuts, shown by the heavy lines, are chosen to reach infinity and divide this into four regions. Thus one obtains the fundamental domain shown in part **(b)**. The identifications a and b are shown as arrows. The lines of these arrows are also the minimal geodesics between the lines that are to be identified. In the identified manifold these are closed geodesics, as shown in part **(a)**. The possible geometries are characterized by the lengths of these two closed geodesics, and the angle between them (shown here as 90°)

ing trousers and analogous asymptotic regions. For example, the $k = 1, g = 1$ geometry can be represented by eliminating two of the horizon geodesics of the trousers octagon and extending the adjacent sides to infinity. This region is then bounded by six geodesics, four of which have one end at infinity. This fundamental domain, bounded by geodesics, is of course not unique. We can cut it into pieces and re-assemble it in a different way [17], or we can cut the original space along some geodesics (not necessarily those of the trousers decomposition) only until it becomes one simply connected piece. If we can lay these geodesics so that they start and end at infinity and therefore do not cross we obtain a simple fundamental region bounded only by complete geodesics. Figure 12a shows the two geodesic cuts necessary for the case of our example of Fig. 11a, and the fundamental domain so obtained is seen in Fig. 12b. The pattern of tiling for this case is identical to that of Fig. 10, but the labeling is different. For example, rather than three horizon words there is only one, $abAB$, corresponding to the existence of only one horizon in the identified manifold.

Out of trousers only one can construct locally AdS initial values that contain no asymptotically AdS region at all. Such compact spaces can be interpreted as closed universes, and for lack of other physical content they can be considered to contain several black holes, associated with the horizons that were glued together in the construction. (Of course these horizons and black holes are only analogies, for example there are no observers that see them as black, i.e. of

infinite redshift.)

Our reasoning about the number of parameters that specify a k -black-hole geometry can be generalized to the case that the internal geometry has genus g . If we cut off two asymptotic AdS regions and identify the two horizons that go with them, we decrease k by two and increase g by one. The number of parameters does not change: we lose one mass parameter, since the masses of the two horizons that will be identified have to be equal, but we gain one rotation parameter which specifies with what shift the horizons are to be identified. Thus from the formula in section 2.4 we find that the (orientable) time-symmetric initial states of genus g and k asymptotic AdS regions form a $(6g + 3k - 6)$ -dimensional Teichmüller space. If this number is non-positive, no state of that type is possible. (However, the formula cannot be applied to the time-symmetric BTZ initial state itself: it has one free parameter, the mass m , but no integral value of k makes the formula valid; the BTZ state is not a multi-black-hole geometry in the sense of this section.) For example, if we want a single exterior region ($k = 1$) we need a genus of at least $g = 1$ (Fig. 12). Here the number of parameters is $6g + 3k - 6 = 3$, for example the minimal distances (lengths of closed geodesics a and b) for each of the two identifications, and the angle between these geodesics. It is clear from the figure that these distances must be large enough, and the angle close enough to a right angle, that an asymptotic region remains in Fig. 12b. (If the geodesics crossed and formed a quadrilateral, there would be an angle deficit at the crossing point, which could be interpreted as a toroidal universe that is not empty, containing one point particle.)

The formula for the number of free parameters tells us that there is no time-symmetric torus ($k = 0, g = 1$) initial state. However, all topologies of higher genus or with at least one asymptotic AdS region do occur; and the spatial torus topology does occur among all locally AdS spacetimes, for example as Eq (7) for $r^2 < \ell^2$ with ϕ and t periodically identified — the analog of a closed Kantowski-Sachs universe.

3 Time Development

The identifications used on a time-symmetric surface of AdS space to generate black hole and other initial values have a unique extension to all of AdS space, and thus define a unique time development (even beyond any Cauchy horizon). A fundamental domain in 3-dimensional AdS space can be generated by extending normal timelike geodesics from the geodesic boundaries of the two-dimensional fundamental domain on the initial surface. Due to the negative curvature of AdS space such *timelike* geodesics accelerate towards each other and will eventually cross. Such crossing of fundamental domain boundaries is the space-time analog of a conical singularity. A prototype of this is the “non-Hausdorff singularity” of Misner space [6]. Although not a curvature singularity, these points are considered not to be part of the space-time. This in turn provides an end of \mathcal{F} and hence the possibility of a black hole horizon.

A metric for the time development of the finite part of any multi-black-

hole or multiply-connected time-symmetric initial geometry is provided by Eq (10) when we replace the expression in the bracket by the initial multi-black-hole metric. The result is a metric adapted to free-fall observers, and it shows that they all reach the singularity after the same proper time, $\tau = \pi\ell/2$, when the \cos^2 factor vanishes. (This can be seen geometrically from Fig. 4a, where geodesics are intersections with planes through the origin, and the collapse time is one quarter of the period around the hyperboloid.) But these coordinates do not cover the time development of conformal infinity (cf. the dotted curves in Fig. 2).

A more complete picture emerges from the continuation of the identification group to AdS spacetime, for example via the embedding of AdS space according to Eq (2). In the embedding of the initial surface in the 3-dimensional Minkowski space $V = 0$, each identification corresponds to a Lorentz “rotation” about some (spacelike) axis A . This is uniquely extended to an $SO(2,2)$ “rotation” of the four-dimensional embedding space by requiring that the V -axis also remain invariant; that is, we rotate by the same hyperbolic angle about the A, V plane. This plane intersects the AdS space (2) in a spacelike geodesic of fixed points. All such geodesics from all the identifications are to be considered singularities after the identifications are made, so they are not points in the identified spacetime.

Three-dimensional pictures that include conformal infinity and all of the singularities can be had in sausage and in stereographic coordinates, Eqs (5) and (14). Because all timelike geodesics starting normally on a time-symmetric initial surface collapse together to a point C , all the totally geodesic boundaries of the fundamental domain also meet at C , forming a tent-like structure with a tip at C . Their intersections may be timelike or spacelike. If an intersection is timelike, the sides typically intersect there at a right angle “corner,” and the intersection passes through the initial surface. If the initial geometry is smooth, such intersections are innocuous.¹⁰ Spacelike intersections are called “folds” of the tent, and they are the geodesics of fixed points, which likewise meet at C .¹¹

The tent has a simple, pyramid shape in a stereographic mapping centered at C . Since all geodesics through the center of the map are represented by straight lines in such a map, the sides of the tent are timelike planes (that is, linear spaces in stereographic coordinates), and the folds are spacelike straight lines. Figure 13 shows a tent with no corners but four folds. This can be the spacetime fundamental domain for the $k = 3, g = 0$ three-black-hole of Fig. 10 or for the $k = 1, g = 1$ toroidal black hole of Fig. 12, depending on the identification rule. In the three-black-hole case two of the folds, on opposite sides, are fixed points of the identifications a and b of Fig. 10 that generate the group. The other two folds are fixed points of ab and of ba . For the toroidal black hole the fixed points of a and of b of Fig. 12 are not folds, they would be horizontal

¹⁰We have not encountered such corners in our pictures, but they must appear in spaces composed only of trousers, for example in the time development of a $k = 0, g = 2$ surface that can be represented by a right-angled octagon on the Poincaré disk, as in Fig. 3b of [17].

¹¹The reason that corners can be regular and but folds are not is that four corners can be put together to make a line without angle deficit, but no finite number of folds can eliminate the Misner-space singularity.

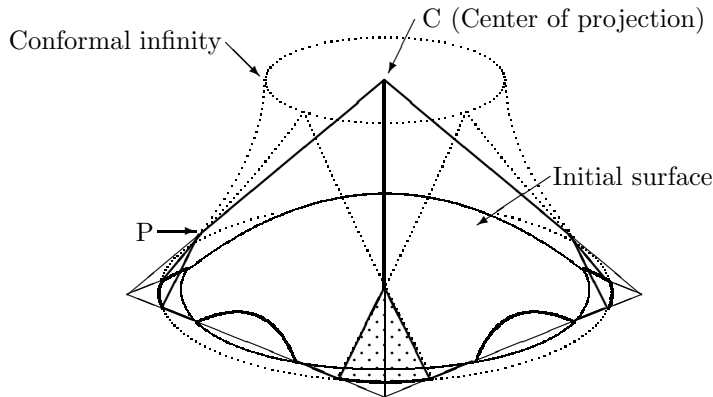


Figure 13: The identification surfaces near the collapse point C in stereographic coordinates. AdS spacetime is the interior of the lightly dotted hyperboloid. The hyperboloid itself represents conformal infinity. The initial surface is a Minkowski hyperboloid (like that of Fig. 5) and in that sense is shown in its true metric. The triangular regions on the infinity hyperboloid, one of which is dotted, are the part of \mathcal{F} that can be shown in this coordinate neighborhood

lines through the tip of the tent. Instead the folds are fixed points of $aba^{-1}b^{-1}$ and its three cyclic permutations. In each case the folds are fixed points of transformations associated with a horizon. All the other fixed points lie outside of the fundamental domain.

Because the stereographic picture is centered at a particular time, it can be misleading in that it does not exhibit the time symmetry about the initial surface, nor the early history before the time-symmetric moment. The time-independent sausage coordinates are more suitable for the global view of a black hole spacetime. Since the BTZ black hole (Fig. 14a) involves only one identification, its fundamental domain has only one geodesic of fixed points to the future of the initial surface, the $r = 0$ line in Fig. 2a. The sides of the tent are the surfaces $\phi = 0$ and $\phi = 2\pi$. Fig. 14b is the sausage coordinate version of Fig. 13.

Since folds are spacelike they extend to infinity, and therefore the initial fundamental domain must also have asymptotic regions. Conversely, the tent of an initial state without asymptotic regions has only corners and a tip but no folds: any closed time-symmetric AdS universe always collapses to a point in the finite time $\pi\ell/2$.

The holes in the tent are important for the black hole interpretation, for they are the regions at infinity \mathcal{F} . The edges of the holes of course disappear once the identifications are made, and the only remaining boundaries of \mathcal{F} appear as points such as those marked P in the figure. The backwards lightcone from P is the boundary of the past of \mathcal{F} , i.e. the horizon. It surrounds the singularity whose end is P . It is now clear that all the initial configurations that have a

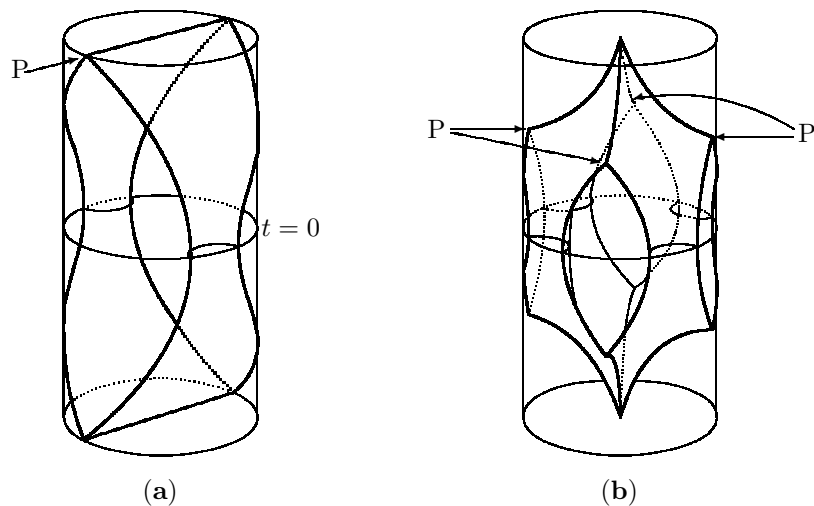


Figure 14: Fundamental regions and their boundary “tents” in sausage coordinates, for (a) the BTZ black hole and (b) a three-black-hole or toroidal black hole configuration

horizon in the sense of section 2.4 do have spacetime horizons and hence are black holes: a horizon word extended to spacetime is an identification that has fixed points along some fold of the tent-shaped boundary of the spacetime fundamental domain. The intersection of the fold with conformal infinity is an endpoint of a \mathcal{S} , and the backwards lightcone of that endpoint is the spacetime horizon.

For a given fold we can consider a region in the fundamental domain sufficiently near infinity (spatially) and the fold (temporally) so that the only relevant identification is the one that has fixed points on that fold (because the other identifications would move points out of the region). In that region the spacetime is then indistinguishable from that of a BTZ black hole, and the spacetime horizon behaves in the same way as a BTZ black hole horizon. For example, the backward lightcone from P does intersect the initial surface in the minimal horizon geodesic. As we follow the horizon further backward in time it changes from the BTZ behavior only when it encounters other horizons or another part of itself, coming from another copy of the point P in the fundamental domain. For example, in the toroidal black hole interpretation of Fig. 14, all four openings of the tent are parts of one \mathcal{S} , and there is a single spacetime horizon consisting of the four “quarter” backwards lightcones from the four copies of the point P. As we go backwards in time below the initial surface these lightcones eventually touch and merge and shown in Fig. 15.

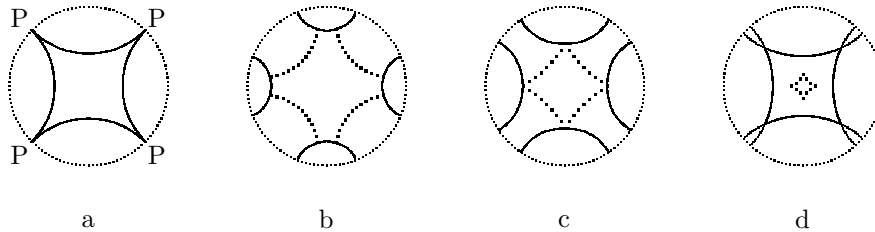


Figure 15: Slices of the sausage in Fig. 14 to show the time development of the horizon. Part a is the latest and part d the earliest sausage time. The geometry of each time slice is the constant curvature space represented by a Poincaré disk. The geodesics shown by solid lines are to be identified as before for the toroidal black hole. Where these geodesics intersect we have a fixed point of some identification, a physical singularity. Slice a is at the sausage time of the end point P of \mathcal{F} . As we go backwards in time, the horizon (dotted arcs of circles) spreads out from those points at infinity. Slice b is the moment of time-symmetry. The horizon remains smooth until slice c, when its different parts meet each other at the identification surfaces. Prior to that time the event horizon has four kinks

3.1 Fixed Points at Infinity

As the above examples of multi-black-hole time developments show, any time-symmetric initial state with an asymptotic region ending at a horizon is isometric to a corresponding region of a BTZ black hole, so that each such region will look like a black hole from infinity for at least a finite time. It is maybe not so clear whether this is also true for the unlimited time necessary for a true black hole, for example because other singularities (fixed points) might intervene. By an interesting method due to Åminneborg, Bengtsson and Holst [18] one can directly find all of the universal covering space of \mathcal{F} from a knowledge of spatial infinity on an initial surface. (The universal covering space gives information about horizons and is natural in many contexts, for example topological censorship questions reduce to existence of certain geodesics in AdS space [17].)

Since our black holes are quotient spaces of AdS space, the covering space of their \mathcal{F} will be a subset of conformal infinity of AdS space. To describe this conformal infinity in a finite way we follow the usual Penrose procedure and multiply the AdS metric by a factor so that the resulting metric is finite in the asymptotic region. An obviously suitable conformal factor in Eq (5) is $(1 - (\rho/\ell)^2)^2$, giving the metric at infinity, $\rho = \ell$,

$$ds_\infty^2 = 4(dt^2 + \ell^2 d\theta^2)$$

This is the flat metric of a cylinder of radius ℓ .

Consider first the covering space of \mathcal{F} of a single black hole in this description, and recall that the identification is a “Lorentz boost” in the embedding space (2). As we apply this transformation n times to get the n th tile of the

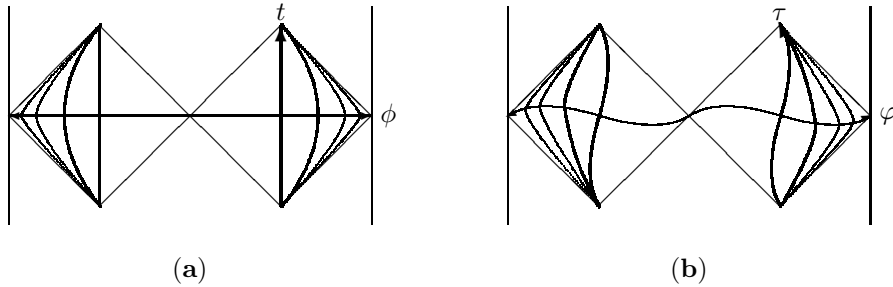


Figure 16: Universal covering spaces of conformal infinity \mathcal{F} for (a) non-rotating, (b) rotating black holes on the conformal infinity cylinder of AdS space. To show the cylinder in this flat picture it has been cut along the vertical lines, which are to be identified with each other in each part of the figure. The angle ϕ resp. φ runs from $-\infty$ to $+\infty$, in the direction of the arrow, in each of the diamond-shaped regions. The intersection of the fundamental domain with conformal infinity of AdS space is shown by the heavier boundaries. These boundaries are at the values 0 and 2π of ϕ resp. φ . A few of the tiles obtained by the isometries that change these angles by $2\pi n$ are shown for positive multiples n . In the limit $n \rightarrow \pm\infty$ the tiles converge to the null boundaries of the two diamond-shaped regions. These null boundaries intersect on the initial surface ($t = 0$ resp. $\tau = 0$) at the $n \rightarrow \infty$ limit at conformal infinity of the initial surface, and they end in the future at the end of \mathcal{F}

covering space, we are boosting the fundamental domain to the limiting velocity, and since the identification boundaries are timelike in our description, they become two null surfaces in the limit $n \rightarrow \pm\infty$. These null surfaces (called “singularity surfaces” in [19]) are then of course invariant under the identification transformation. Hence, if $\mathbf{K} = \partial/\partial\phi$ is the Killing vector corresponding to the identification, these surfaces are described by $\mathbf{K}^2 = 0$. They intersect where the vector \mathbf{K} itself vanishes, that is at the fixed points at infinity on the initial surface and at the singularity inside the black hole.

The intersection of these surfaces with conformal infinity of AdS space is the boundary ($n \rightarrow \infty$) of the covering space of \mathcal{F} . To find it we only need to draw null lines from the endpoints of the horizon at $t = 0$ toward each other (Fig. 16a). Their future intersection is the nearest future fixed point to this initial surface, it is the end of \mathcal{F} , and the covering space of \mathcal{F} is the diamond-shaped region between the future and past null lines. Furthermore the future null lines are also the intersection of the covering space of the horizon with conformal infinity, since the horizon is the backward null cone from the end of \mathcal{F} . Thus a knowledge of the initial fixed points gives us the “holographic” information about the exterior and the horizon of the black hole.

The situation for time-symmetric multi-black-holes is similar, except that the construction yields an infinite number of copies of the covering space of \mathcal{F} . We saw in Fig. 10 that each horizon word has two fixed points at spatial infinity.

Each such pair yields a diamond-shaped region for which the transformation of its horizon word looks like that of Fig. 16a, and which is free of fixed points.

4 Angular Momentum

In the metric (18) for the static BTZ black hole, introduce new coordinates T, φ, R ,

$$\begin{aligned} t &= T + \left(\frac{J}{2m}\right)\varphi \\ \phi &= \varphi + \left(\frac{J}{2m\ell^2}\right)T \\ R^2 &= r^2 \left(1 - \frac{J^2}{4m^2\ell^2}\right) + \frac{J^2}{4m} \end{aligned} \tag{19}$$

where $J < 2m\ell$ is a constant with dimension of length, and define another new constant

$$M = m + \frac{J^2}{4m\ell^2}. \tag{20}$$

In terms of these new quantities the metric (18) may be written as

$$ds^2 = -N^2 dT^2 + N^{-2} dR^2 + R^2 \left(d\varphi + \frac{J}{2R^2} dT\right)^2 \tag{21}$$

where

$$N^2 = \left(\frac{R}{\ell}\right)^2 - M + \left(\frac{J}{2R}\right)^2.$$

The metric (21) now looks like a (2+1)-dimensional analog of the metric for a black hole that carries angular momentum. Although metric (21) was obtained by a coordinate transformation from (18) and is therefore locally isometric to the latter (as all of our spaces are locally isometric to AdS space), it differs in its global structure: we have silently assumed that the new metric (21) is periodic with period 2π in the *new* angular variable φ , rather than in the old variable ϕ . This means, in coordinate-independent language, that we have changed the identification group that creates this new spacetime from AdS space. As for the non-rotating BTZ black hole, the new group for this “single” rotating black hole is still generated by all the powers of a single isometry of AdS space, but this isometry does not leave invariant a totally geodesic spacelike surface of time symmetry. The surface $T = \text{const}$ that is obviously left invariant by a displacement of φ is twisted, as measured by its extrinsic curvature, and this is one indication of the global difference from the static metric.

When only the one new coordinate φ changes by 2π , the old coordinates of (18) change by

$$t \rightarrow t + \frac{\pi J}{m} \quad \phi \rightarrow \phi + 2\pi. \tag{22}$$

A change in either t or ϕ is of course an isometry of the metric (18), and because t and ϕ are coordinates, the two changes commute. The identification for a rotating black hole involves the two isometries applied simultaneously. Either one is a “boost” about an axis of fixed points; the change in ϕ has fixed points in the future, at $r = 0$, and the change in t has fixed points at $r = \ell\sqrt{m}$, the horizon of (18).¹² The combination of the two does not have any fixed points at all (either one moves points on the fixed axis of the other in the direction of the axis): the length R^2 of the corresponding Killing vector $\partial/\partial\varphi$ vanishes where the vector is null but not zero, since its scalar product with the finite $\partial/\partial T$ is the finite constant J . Earlier we argued that a spacelike set of fixed points of the identification isometry becomes a kind of singularity after the identification, and its removal from the spacetime gave us the end of \mathcal{F} and associated horizon. What happens when we do not have this singularity?

4.1 Is it a Black Hole?

The geometry of metric (21) — more properly speaking, the geometry of its analytic extension, or of AdS space identified according to the $\varphi \rightarrow \varphi + 2\pi$ isometry exhibited by this metric — satisfies the definition of a black hole if we are somewhat creative about the definition of “singularity.” We expect the singularity to occur at $R = 0$, but because there are no fixed points, the identified spacetime is regular there, and can be continued to negative R^2 . But then the closed φ -direction becomes timelike, hence the spacetime has a region of closed timelike lines. We shall follow the usual practice to regard these sufficiently unphysical that they should be eliminated from the spacetime, like a singularity, and confine attention to $R > 0$.

Our spacetime then ends at the singularity surfaces where the square of the Killing vector $\partial/\partial\varphi$ vanishes, $R^2 = 0$. The corresponding r^2 of Eq (20) is negative. We recall from Sect. 2.1 that this occurs on two timelike surfaces in a region where ϕ is timelike, unlike the non-rotating black hole whose singularity occurs on the spacelike line $r = 0$. Since there is a singularity-free region between the two singularity surfaces, not all timelike lines that “fall into the black hole” (cross the horizon) end at the singularity, they can escape through the hole left open by the singularity surfaces, as is the case in a three-dimensional Kerr black hole. However, at conformal infinity the difference between R and r disappears, the two singularity surfaces come together at the point where the spacelike line $r = 0$ meets conformal infinity.

Thus the covering space of \mathcal{F} for the rotating black hole looks the same as that of the non-rotating one that corresponds to it via Eq (20), only the identification is different, as shown in Fig. 16b. We see that \mathcal{F} has an endpoint, there is a horizon, and the identified spacetime is a black hole.

We can recognize a (rotating) black hole in a spacetime by the presence of a closed, non-contractible spacelike geodesic γ . If we have such a γ we consider all

¹²Since these isometries are also isometries of the periodically identified embedding (2), each axis of fixed points is really repeated an infinite number of times in AdS space itself.

spacelike geodesics that start normal to γ . We assume that these can be divided into two types, which we might call right-starting and left-starting (with respect to an arbitrarily chosen direction of γ). If all geodesics of one type reach infinity, then they cover the outside of a black hole. In this region the totally geodesic timelike surfaces normal to γ are surfaces of constant ϕ . Within these surfaces one can introduce coordinates so that the metric takes the form (21). (If the normals to those surfaces, not at γ , also integrate to closed curves after one circuit of γ , we have $J = 0$.)

4.2 Does it rotate?

The asymptotically measurable properties of (2+1)-dimensional black holes can be defined in various way, for example from the ADM form of the Einstein action, as the conserved quantities that go with the Killing vectors $\partial/\partial t$ and $\partial/\partial\varphi$, as the Noether charges associated with t - and φ -displacements, and so on [20, 1]. All of these yield M as the mass and J as the angular momentum.

J can also be measured “quasi-locally” in the neighborhood of the horizon. We find an extremal closed spacelike geodesic (corresponding to $r = \ell$) and parallel transport an orthogonal vector around this geodesic. According to Eq (22) the hyperbolic “holonomy” angle between the original and rotated vectors is $\pi J/m\ell$.

4.3 Multiple Black Holes with Angular Momentum

It is fairly straightforward to extend the methods of section 2.4 to obtain metrics with several asymptotic regions, or with non-standard topologies, that have angular momentum as measured in these asymptotic regions; the main difference is that we will deal with spacetimes rather than initial values. Our aim is only to show that rotating multi-black-holes are possible, and to indicate what the free parameters are.

We start with the time development of a time-symmetric n -black-hole space-time, described by doubling as in Fig. 9a. The identifications now take place on timelike, totally geodesic identification surfaces, which are the time development of the geodesics reaching infinity in Fig. 9a. We change the identifications by introducing some “twist” as in Eq (22) along the initial horizons, between surface 1 and 2, 2 and 3 . . . $n - 1$ and n . Thereby the new identification between surfaces n and 1 is also defined, so we can choose $n - 1$ angular momentum parameters. If these are not too large, there is a *spacelike* extremal¹³ geodesic γ between surfaces n and 1 that is smoothly closed after doubling. One set of spacelike normals to γ will reach infinity, because they do so in the AdS covering space, so the n th region is also a black hole.

Fig. 17 illustrates this for a simple, very symmetric three-black-hole configuration in the fundamental domain description (the time development of a figure like Fig. 8b). Poincaré disk D1 and the four geodesics drawn on it are

¹³This means that the total length of γ , *after* the doubling identification, is extremal also when the endpoints are varied within the surfaces n and 1.

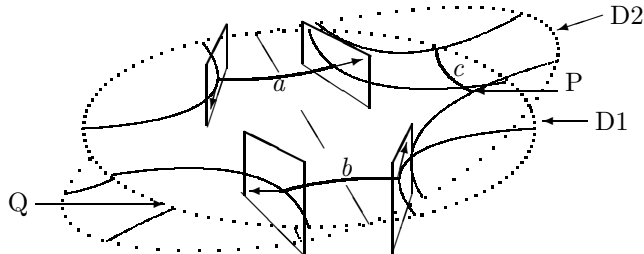


Figure 17: Stereographic picture of the identifications among four identification surfaces in AdS space that lead to a multi-black-hole geometry where two of the black holes have angular momenta

seen at an oblique angle. The geodesics are extended by orthogonal geodesics out of the surface D1 to form the totally geodesic identification surfaces in a three-dimensional stereographic projection of AdS space. These hyperboloids are not drawn because they would obscure the rest of the picture. Poincaré disk D2 is a “boost” of D1, and the geodesics on it are intersections with the hyperboloids. The two surfaces connected by geodesic a are to be identified, and likewise for geodesic b , but each with a twist as indicated by the arrows. (Arrow tails are identified with tails, and arrow heads with heads). The lengths of a and b are equal and the amount of twist J along them is equal and opposite¹⁴ so that the figure is symmetric under 180° rotation about the dashed line, and reflection symmetric about a plane orthogonal to the dashed line at its midpoint. Geodesics a and b are then by construction associated with two rotating black holes (the regions extending to infinity toward the front and back of the picture). The third black hole is made of the regions extending to infinity to the right and to the left of the picture, which form one connected region after the identification is made. Among curves that encircle this black hole we find the extremal one (described by this horizon “word” $aba^{-1}b^{-1}$). This is geodesic c , lying in D2, and a geodesic d symmetrically placed but hidden behind D1. From the symmetry it is clear that the twist around the union of c and d vanishes, so the third black hole has zero angular momentum.¹⁵

At conformal infinity each of the asymptotic regions look like those shown in Fig. 16, but for the case with angular momentum these regions are arranged

¹⁴By “opposite” we mean that one twist is right-handed and the other is left-handed. Although the black holes live in different asymptotic regions, the sign as well as the magnitude of J can be compared between such black holes.

¹⁵The hyperbolic angle between D1 and D2 is determined by J . To see this one may conversely start with a choice of this hyperbolic angle and find the minimal geodesics c and d within D2. Then the bottom right arrow, for example, is turned out of the surface D1 so that a geodesic to which it is tangent passes through P, the foot of geodesic c . Similarly the left bottom arrow is tangent to a geodesic bound for Q, the foot of the hidden geodesic d .

about a “jagged” line, unlike the line $t = 0$ in the non-rotating case [18].

To obtain more than three black holes with angular momenta we can either start with a time-symmetric configuration of n black holes and introduce $n - 1$ angular momenta as outlined above; or we can more generally, as in section 2.5, cut off asymptotic “legs” from pairs of three-black-holes and match across the extremal geodesic, provided we match the size and the angular momentum associated with the extremal geodesics. When we make a configuration with n asymptotic regions in this way we therefore have $n - 1$ independent angular momentum parameters.

Configurations constructed in other ways do not have to follow this formula. For example, the toroidal black hole with $n = 1$ constructed as in Fig. 12 can be given angular momentum [18].

5 Conclusions

We have seen that a considerable variety of black hole and multiply-connected spacetimes can be constructed by cutting a region out of anti-de Sitter space and identifying the cuts in various ways. Many of the properties, such as horizon structure and topological features of the time-symmetric spacetimes, have been investigated in detail. Comparatively little beyond existence is known about the spacetimes with angular momentum (but see [18]).

References

- For an extended list of references through 1994, see Carlip, S. (1995) The (2+1)-dimensional black hole. *Class. Quant. Grav.* **12**, 2853-2880
- [1] Bañados, M., Teitelboim, C., Zanelli, J., (1992) The black hole in three-dimensional space-time. *Phys. Rev. Lett.* **69**, 1849-1851; Bañados, M., Henneaux, M., Teitelboim, C., Zanelli, J. (1993) Geometry of the (2+1) black hole. *Phys. Rev. D***48**, 1506-1525
 - [2] Mess, G. (1990) Lorentz spacetimes of constant curvature. IHS preprint
 - [3] Morrow-Jones, J., Witt, D. (1993) Inflationary initial data for generic spatial topology. *Phys. Rev. D* **48**, 2516-2528
 - [4] 't Hooft, G. (1993) Classical n particle cosmology in (2+1)-dimensions. *Class. Quant. Grav.* **10**, Suppl. 79-91.
 - [5] See for example Strominger, A. (1994) Les Houches lectures on black holes. hep-th/9501071
 - [6] Misner, C. (1967) Taub-NUT space as a counterexample to almost anything. In *Relativity Theory and Astrophysics I*, ed. J. Ehlers, Lectures in Applied Mathematics **8**, 160-169

- [7] For a recent exposition of asymptotically flat black holes see Heusler, M (1996) *Black Hole Uniqueness Theorems*. Cambridge University Press; for the asymptotically AdS case see [20]
- [8] Benedetti R., Petronio, C. (1992) *Lectures on Hyperbolic Geometry*. Springer, Berlin Heidelberg
- [9] Carlip, S (1998) *Quantum gravity in 2+1 dimensions*. Cambridge University Press
- [10] Holst, S. (1996) Gott time machines in anti-de Sitter space. *Gen. Rel. Grav.* **28**, 387-403; Åminneborg, S., Bengtsson, I., Holst, D., Peldán, P. (1996) Making anti-de Sitter black holes. *Class. Quant. Grav.* **13**, 2707-2714
- [11] Li, Li-Xin (1999) Time machines constructed from anti-de Sitter space. *Phys. Rev. D* **59**, 084016
- [12] Bachmann F. (1973) *Aufbau der Geometrie aus dem Spiegelungsbegriff*. Springer, Berlin Heidelberg
- [13] Flamm, L (1916) Beiträge zur Einsteinschen Gravitationstheorie. *Phys. Z.* **17**, 448-454, or see Misner, C., Thorne, K., Wheeler, J., (1973) *Gravitation* (p. 614). Freeman, San Francisco; Marolf, D. (1999) Space-time embedding diagrams for black holes. *Gen. Rel. Grav.* (to appear), gr-qc/9806123
- [14] Brill, D. (1996) Multi-black hole geometries in (2+1)-dimensional gravity. *Phys. Rev. D* **53**, 4133-4176; Steif, A. (1996) Time-Symmetric initial data for multi-body solutions in three dimensions. *Phys. Rev. D* **53**, 5527-5532
- [15] Susskind, L. (1995) The world as a hologram. *J. Math. Phys.* **36**, 6377-6396; Witten, E. (1998) Anti-de Sitter space and holography. *Adv. Theor. Math. Phys.* **2**, 253-291
- [16] Holst, S. (1997) On black hole safari in anti-de Sitter space. *Filosofie Licentiaexamen, Dept. of Phys., Stockholm Univ.*
- [17] Åminneborg, S., Bengtsson, I., Brill, D., Holst, D., Peldán, P. (1998) Black holes and wormholes in 2+1 dimensions. *Class. Quant. Grav.* **15**, 627-644
- [18] Åminneborg, S., Bengtsson, I., Holst, S (1999) A spinning anti-de Sitter wormhole. *Class. Quant. Grav.* **16**, 363-382
- [19] Holst, S., Peldán, P. (1997) Black holes and causal structure in anti-de Sitter isomorphic spacetimes. *Class. Quant. Grav.* **14**, 3433-3452
- [20] Carlip, S., Gegenberg, J., Mann, R., (1995) Black holes in three-dimensional topological gravity. *Phys. Rev. D* **51**, 6854-6859; Abbott, L., Deser, S. (1982) Stability of gravity with a cosmological constant. *Nucl. Phys. B* **195**, 76; Brown, J., Creighton, J., Mann, R. (1994) Temperature, energy and heat capacity of asymptotically anti-de Sitter black holes. *Phys. Rev. D* **50**, 6394-6403